Complex Analysis of Askaryan Radiation: UHECR Reconstruction with Askaryan Radio Array

Jordan C. Hanson* and Damian Ibañez-Rodriguez
Department of Physics and Astronomy, Whittier College
(Dated: February 27, 2026)

Ultra-high energy cosmic rays (UHECR) can produce relativistic cascades that emit radio-frequency (RF) pulses in the 10-1000 MHz bandwidth via two distinct effects: the geomagnetic effect, and the Askaryan effect. The geomagnetic effect occurs when the magnetic field of the Earth causes cascade charges to form a transverse current that radiates linearly polarized radiation aligned with the Lorentz force direction. The Askaryan effect is caused by the net negative charge excess in the cascade that radiates linearly polarized radiation along the Cherenkov cone. When UHECR cascades enter solid, RF transparent matter at altitudes where the cascade develops, Askaryan radiation can propagate through the solid matter to RF detectors. The Askaryan Radio Array (ARA) at the South Pole has observed 13 UHECR candidates in precisely this fashion. We present an analytical model that confirms the events are UHECRs. The model includes the Askaryan effect and the ARA RF channel response. The coherently summed waveforms (CSWs) from the UHECR candidates match our model with correlation coefficients between 0.69 and 0.86, and with minimal fractional power differences. From the fit between model and data, we extract the Askaryan pulses.

Keywords: Ultra-high energy neutrino; Askaryan radiation; Mathematical physics

I. INTRODUCTION

UHECR cascades produce RF pulses via the geomagnetic and Askaryan effects, and these pulses have been used to study UHECR properties [1, 2]. Detectors with RF channels sensitive to RF pulses from UHECRs add complementary data for event reconstruction to traditional ground-based muon and fluorescence detectors. UHECR candidate events have now been presented by the Antarctic Ross Ice Shelf Antenna Neutrino Array (ARIANNA), ARA, and Radio Neutrino Observatory Greenland (RNO-G) collaborations [3–5]. In ARA, the contribution from the Askaryan effect dominates the observed RF pulses. Due to the unique location of ARA at the South Pole, the contribution from the Askaryan effect dominates the observed RF pulses. The South Pole is 2800 meters above sea level, and the thin atmosphere allows UHECR cascades to develop near the altitude of the ARA RF detection channels. As charged particles from the UHECR cascade enter the ice, the negative excess charge radiates collectively in the 0.1-1 GHz bandwidth.

Within the genre of calculations that predict the properties of RF pulses from UHECRs and ultra-high energy neutrinos (UHE-ν), there are three classes of models. First, Monte Carlo programs may be used to track each particle and corresponding RF emission within the cascade. These are known as full Monte Carlo, or *full-MC calculations* [6–8]. Second, there are formalisms in which the analytic vector potential corresponding to the radiating charge is convolved with the simulated cascade profile. These are called *semi-analytic calculations*, and have been used to predict the RF pulses from UHE-ν interacting in Antarctic and Greenlandic ice [9–11]. Finally, there are *fully analytic* calculations that derive the UHECR or UHE-ν signal from classical electrodynamics. Examples of such models are Ralston and Buniy (RB2001) [12], Hanson and Connolly (HCRB2017) [13], and Hanson and Hartig (HHH2022) [14].

One key advantage of fully analytic Askaryan calculations is that they can be fit to raw data from Askaryan-class detectors. A prediction for the voltage trace from an RF detection channel is produced by convolving the analytic Askaryan model with an accurate model of the RF channel response. Analytic voltage traces can be matched to the observed voltage traces by maximizing the correlation coefficient from cross-correlation while tuning parameters like the Askaryan pulse width. Recently, Hanson and Hartig presented evidence that the HH2022 model, when convolved with an RF channel model, produces analytic voltage traces that match voltage traces from UHE-ν signals in NuRadioMC [11]. This technique can be used to reject several years of thermal noise backgrounds in detectors like ARA and RNO-G (HH2026) [15]. Further, once the match between observed and analytic voltage trace is optimized, the Askaryan electromagnetic pulse can be extracted based on the fit parameters. In this work, we show that the HH2026 procedure matches the voltage traces from 13 UHECR candidate events observed by ARA [4].

The remaining sections of this work are organized as follows: in Sec. II, we define units, functions, operations on functions, and notational conventions. In Sec. III, we review the necessary portions of the design of the Askaryan Radio Array detector, including the properties of the RF channels. In Sec. IV, we present the match between our theoretical voltage traces and the ARA data. Finally, in Sec. V, we summarize our results and indicate future directions of the research.

*Electronic address: jhanson2@whittier.edu

II. UNITS, DEFINITIONS, AND CONVENTIONS

Our goal is to demonstrate a match between a theoretical voltage trace for a UHECR candidate in ARA RF channels, and the observed voltage traces from those same channels. Let the Askaryan *signal* created by the portion of the UHECR cascade radiating in the ice be $s(t)$. Let E_0 be the amplitude in V m^{-1}, t be the time in ns relative to peak emission, and σ_t be the pulse width in ns. According to Eqs. 28 and 9 and from [14, 15], respectively, $s(t)$ is

$$s(t) = -E_0 t e^{-\frac{1}{2}(t/\sigma_t)^2} \tag{1}$$

To predict a voltage trace from an RF dipole channels in ARA, $s(t)$ must be convolved with $r(t)$, the RF channel response. Let R_0 be the amplitude of the response, with units of m ns^{-1}, f_0 be the resonance frequency of the dipole in GHz, and γ be the exponential decay constant in GHz. According to Eq. 31 from [15], $r(t)$ is

$$r(t) = R_0 e^{-2\pi\gamma t}\cos(2\pi f_0 t) \tag{2}$$

The predicted voltage trace is given by the convolution of $s(t)$ and $r(t)$, denoted $s(t) * r(t)$. The convolution is defined as:

$$s(t) * r(t) = \int_{-\infty}^{\infty} s(t-\tau) r(\tau) d\tau \tag{3}$$

Let $u(t)$ represent the Heaviside step function. According to Eq. 55 from [15], $s(t) * r(t)$ becomes

$$s * r = -E_0 R_0 \int_{-\infty}^{\infty} (t-\tau) e^{-\frac{1}{2}\left(\frac{t-\tau}{\sigma_t}\right)^2} \Re\left\{e^{2\pi j f_0 \tau} e^{-2\pi\gamma\tau}\right\} u(\tau) d\tau \tag{4}$$

The Heaviside step function is introduced to ensure causality. When the voltage trace is predicted with $s(t) * r(t)$, the result must be matched to the data $d(t)$ from the RF channels. The RF channels have fixed, measured values for γ and f_0. The match between $s(t) * r(t)$ and $d(t)$ is achieved by tuning σ_t to maximize the peak value of the cross-correlation, $d(t) \star (s(t) * r(t))$. Cross-correlation is defined for real signals as:

$$f(t) \star g(t) = \int_{-\infty}^{\infty} f(\tau) g(t+\tau) d\tau \tag{5}$$

The algorithm used to compute the cross-correlation in this analysis is `scipy.signal.correlate`. To maximize the signal to noise ratio (SNR) of UHECR data, traces from multiple channels are combined to form the *coherently summed waveform* (CSW). The CSW is computed from a set of traces using the following algorithm: (1) select a reference trace, (2) cross-correlate with the next trace in the set until the cross-correlation is maximized, (3) add the two traces to form a new reference, and (4) repeat until each trace in the set is added coherently to the reference. The CSW is normalized so that the inner product of the trace is one. The theoretical trace is normalized in the same way. Normalized traces lose the voltage units, but retain nanoseconds for the unit of time.

The solution to Eq. 4 was shown in Eq. 61 of [15]. Let $j = \sqrt{-1}$, $x = t/(\sqrt{2}\sigma_t)$, $z = (2\pi j f_0 - 2\pi\gamma)\sqrt{2}\sigma_t$, $w(z)$ be the Faddeeva function of a complex variable, and

$$q = -j\left(x + \frac{z}{2}\right) \tag{6}$$

The solution to Eq. 4 is

$$s * r = -\sqrt{\pi} R_0 E_0 \sigma_t^2 \left(x e^{-x^2} \Re\{w(q)\} - \frac{1}{2} e^{-x^2} \Re\left\{-j\frac{dw(q)}{dq}\right\}\right) \tag{7}$$

A Python3 code was given in [15] to compute Eq. 7. Note that q depends on x, which depends on t. The $s * r$ oscillates at a frequency $\approx f_0$ because the Faddeeva function oscillates with a complex argument. The envelope of $s * r$ rises and falls with the width of $s(t)$, and due to the exponential decay of $r(t)$.

III. THE ASKARYAN RADIO ARRAY

The Askaryan Radio Array consists of five stations deployed near the South Pole designed to detect UHE-ν and UHECR events via the Askaryan effect in Antarctic ice [16–19]. The A5 station utilizes a dedicated RF trigger on the CSW output of a phased array of seven vertically polarized dipoles. The RF phased array trigger boosts the SNR of UHE-ν and UHECR events, and allows for increased sensitivity to rare fluxes of these particles [20]. The ARA UHECR candidates used in this analysis were recorded on the A5 station via the RF phased array trigger. A schematic of the A5 detector is shown in Fig. 1, and the A5 detector parameters are summarized in [16].

The UHECR candidate events were detected with the RF phased array trigger in A5. The proposed event geometry is shown in Fig. 2. The UHECR candidates would normally create both geomagnetic and Askaryan radiation, and geomagnetic radiation usually dominates the total electromagnetic pulse when the detector lies far beneath the cascade [3]. The same claim is made in recent UHECR candidate detections via RNO-G [5], though RNO-G and ARA are situated at high altitudes.

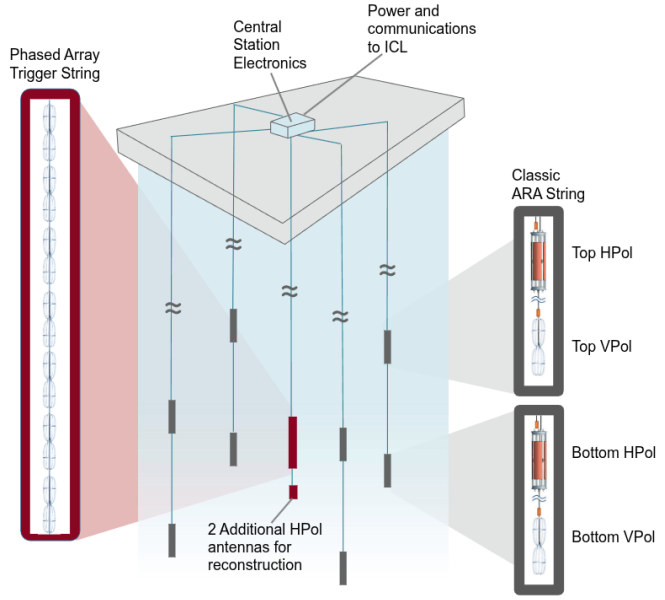

FIG. 1: A general schematic of the A5 station within the Askaryan Radio Array (ARA) detector. The RF phased array trigger string is in the center, surrounded by four reconstruction strings. Strings have both HPol and VPol RF channels. Figure adopted from [16].

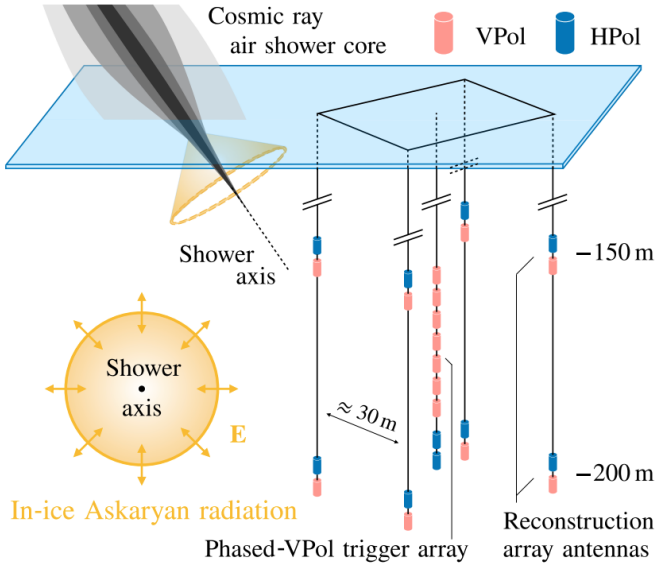

FIG. 2: The proposed UHECR candidate event geometry consists of a high-energy cascade interacting along the shower axis that enters the ice and creates Askaryan radiation. Figure adopted from [16]. Figure adopted from [4].

ID	$\sigma_{t,1}$ (ns)	$\sigma_{t,2}$ (ns)	Δt (ns)	Rel. amp.	ρ
1915-26288	0.6	2.0	25.25	0.08	0.86
1957-13330	0.5	1.8	11.5	0.09	0.74
2171-31805	0.6	1.9	25.25	0.09	0.81
2250-20189	0.7	2.2	24.75	0.09	0.81
2352-85489	0.7	2.1	24.75	0.10	0.84
2375-17342	0.6	1.9	19.0	0.09	0.73
2529-09767	0.7	1.9	25.5	0.11	0.82
2716-58611	0.8	–	–	–	0.84
2782-00106	0.7	2.1	24.5	0.11	0.84
2955-47449	0.5	1.6	25.0	0.03	0.69
2961-98361	0.6	1.9	24.25	0.05	0.80
2978-29412	0.5	1.7	25.5	0.05	0.82
3352-89556	0.5	1.8	25.5	0.05	0.81

At the South Pole, however, geomagnetic radiation is expected to be horizontally polarized due to the vertical orientation of the local magnetic field. The vertically polarized (VPol) RF channels are therefore less sensitive to geomagnetic radiation. Data from the horizontally polarized (HPol) RF channels is not included in our analysis. For the VPol phased array channels, we will show in Sec. IV that geomagnetic radiation is not necessary to explain the observed voltage traces.

1. Calibration of f_0 from data itself
2. Calibration of γ from data itself

IV. RECONSTRUCTION ANALYSIS

1. Waveform reconstruction
   - Present graphs and tabulated results for CSWs by event
   - Present graphs and tabulated results for subsets of channels by event
2. E-field calculations
   - E-field of UHECRs from CSWs
   - E-field of UHECRs from channel subset CSWs

V. CONCLUSION

What did we learn? How to reconstruct the E-field, and the product $\sigma_t \propto a\Delta\theta$ tells us about the event geometry and energy

Appendix A: The appendix

Derivation of the $s * r$, maybe the code to do it

[1] T. Huege and D. Besson, Progress of Theoretical and Experimental Physics **2017**, 12A106 (2017), ISSN 2050-3911, 1701.02987.

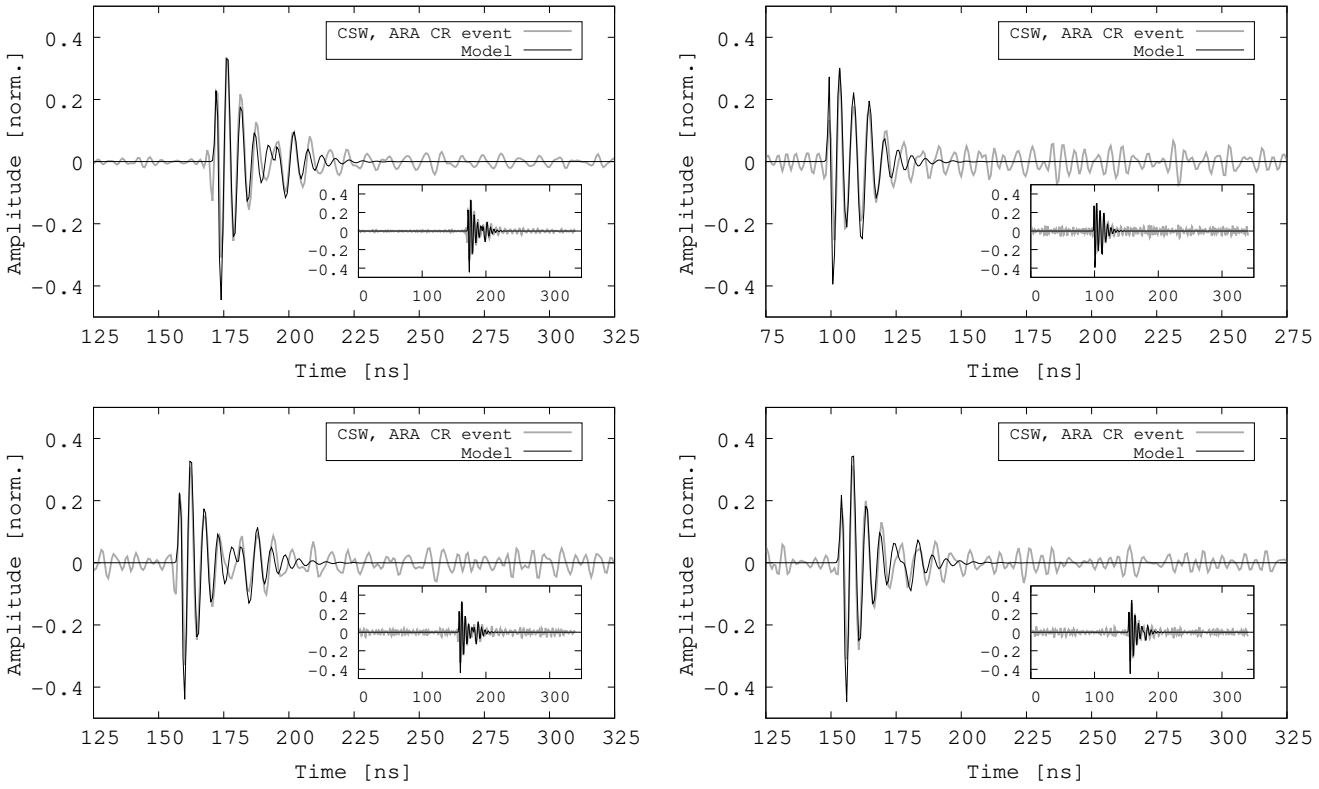

FIG. 3: UHECRs, by ID: (top left) 1915-26288, (top right) 1957-13330, (bottom left) 2171-31805, (bottom right) 2250-20189.

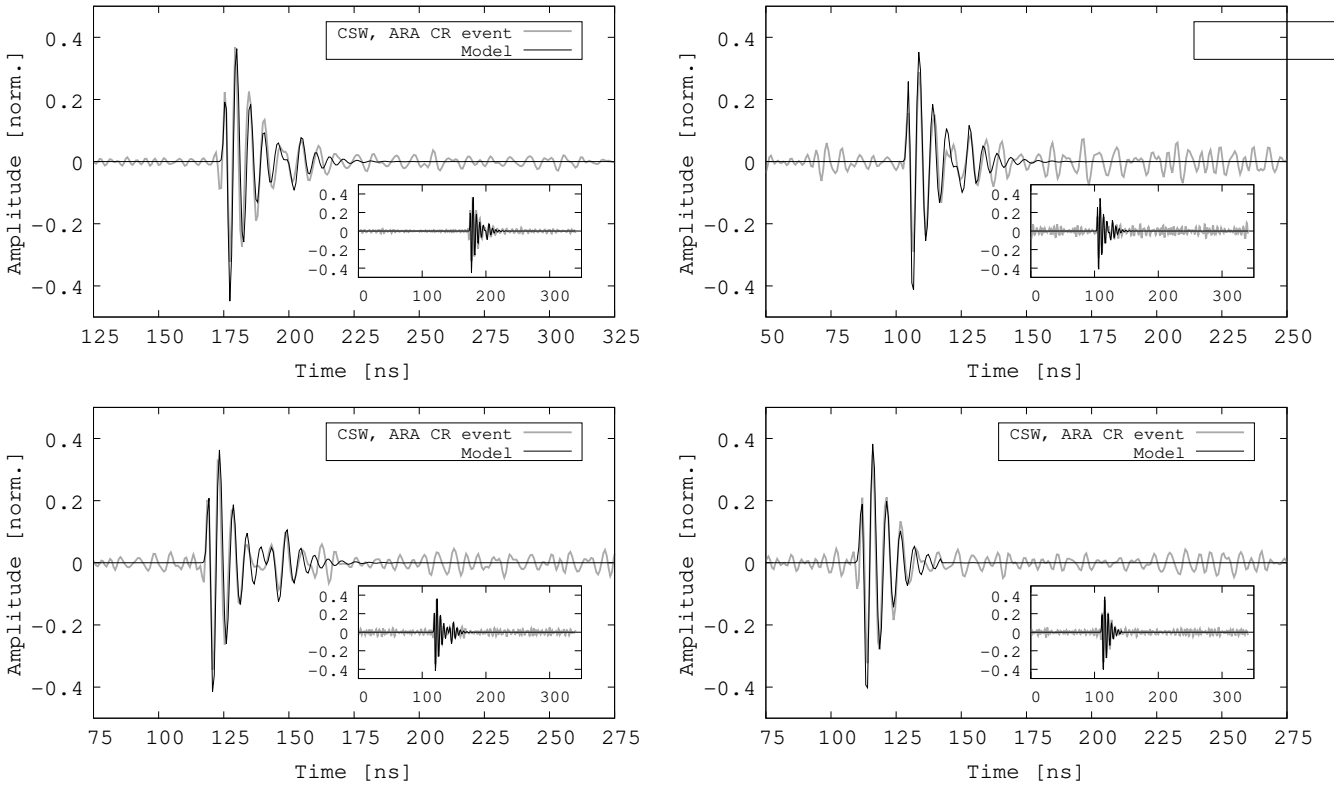

FIG. 4: UHECRs, by ID: (top left) 2352-85489, (top right) 2375-17342, (bottom left) 2529-09767, (bottom right) 2716-58611.

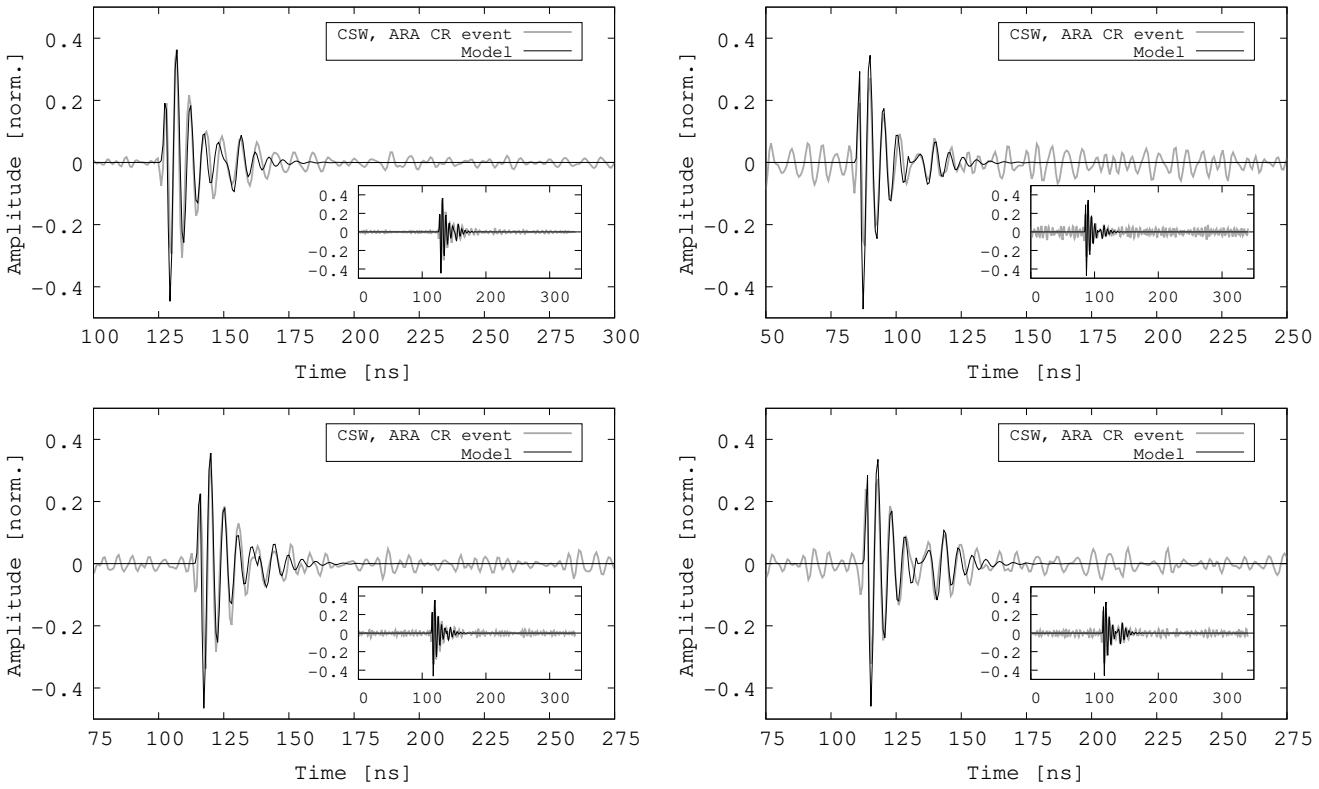

FIG. 5: UHECRs, by ID: (top left) 2782-00106, (top right) 2955-47449, (bottom left) 2961-98361, (bottom right) 2978-29412.

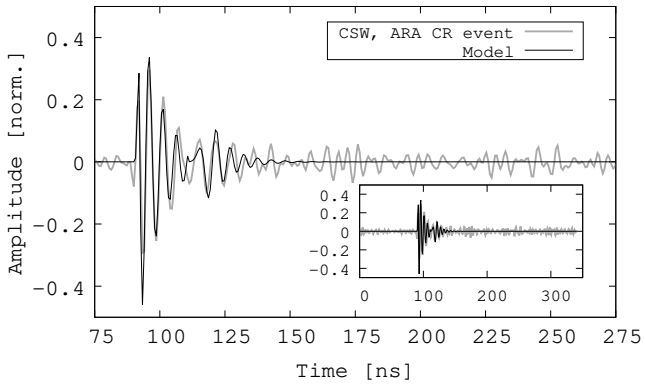

FIG. 6: UHECRs, by ID: 3352-89556

[2] F. G. Schröder, The European physical journal. Special topics **234**, 4957 (2025), ISSN 1951-6355, 2502.19969.
[3] S. Barwick, D. Besson, A. Burgman, E. Chiem, A. Hallgren, J. Hanson, S. Klein, S. Kleinfelder, A. Nelles, C. Persichilli, et al., Astroparticle Physics **90**, 50 (2017), ISSN 0927-6505, 1612.04473.
[4] A. Collaboration, N. Alden, S. Ali, P. Allison, S. Archambault, J. J. Beatty, D. Z. Besson, A. Bishop, P. Chen, Y. C. Chen, et al., arXiv (2025), 2510.21104.
[5] S. Agarwal, J. A. Aguilar, N. Alden, S. Ali, P. Allison, M. Betts, D. Besson, A. Bishop, O. Botner, S. Bouma, et al., arXiv (2025), 2512.17664.
[6] E. Zas, F. Halzen, and T. Stanev, Physical Review D **45**, 362 (1992).
[7] J. Alvarez-Muñiz, C. James, R. Protheroe, and E. Zas, Astroparticle Physics **32**, 100 (2009), ISSN 0927-6505.
[8] J. Alameddine, J. Albrecht, J. Ammerman-Yebra, L. Arrabito, A. Alves, D. Baack, A. Coleman, H. Dembinski, D. Elsässer, R. Engel, et al., Astroparticle Physics **166**, 103072 (2025), ISSN 0927-6505, 2409.15999.
[9] J. Alvarez-Muniz, A. Romero-Wolf, and E. Zas, Physical Review D **84**, 103003 (2011), ISSN 2470-0029, 1106.6283.
[10] J. Alvarez-Muniz, P. M. Hansen, A. Romero-Wolf, and E. Zas, Phys. Rev. D **101**, 083005 (2020), URL `https://link.aps.org/doi/10.1103/PhysRevD.101.083005`.
[11] C. Glaser et al, The European Physical Journal C **80**, 77

(2020), ISSN 1434-6044, 1906.01670.

[12] R. V. Buniy and J. P. Ralston, Physical Review D **65** (2001), ISSN 2470-0029.

[13] J. C. Hanson and A. L. Connolly, Astroparticle Physics **91**, 75 (2017), ISSN 0927-6505.

[14] J. C. Hanson and R. Hartig, Phys. Rev. D **105**, 123019 (2022), URL https://link.aps.org/doi/10.1103/PhysRevD.105.123019.

[15] J. C. Hanson and R. Hartig, arXiv (2026), 2602.21412.

[16] P. Allison, S. Archambault, J. J. Beatty, D. Z. Besson, A. Bishop, C. C. Chen, C. H. Chen, P. Chen, Y. C. Chen, B. A. Clark, et al., Physical Review D **105**, 122006 (2022), ISSN 2470-0010, 2202.07080.

[17] The ARA Collaboration, Physical Review D **102**, 043021 (2020), ISSN 2470-0010, 1912.00987.

[18] P. Allison, J. Auffenberg, R. Bard, J. Beatty, D. Besson, S. Böser, C. Chen, P. Chen, A. Connolly, and J. Davies, Astroparticle Physics **35**, 457 (2012), ISSN 0927-6505, 1105.2854.

[19] The ARA Collaboration, Astroparticle Physics **70**, 62 (2015), ISSN 0927-6505, URL https://www.sciencedirect.com/science/article/pii/S0927650515000687.

[20] J. Avva, K. Bechtol, T. Chesebro, L. Cremonesi, C. Deaconu, A. Gupta, A. Ludwig, W. Messino, C. Miki, R. Nichol, et al., Nuclear Instruments and Methods in Physics Research Section A: Accelerators, Spectrometers, Detectors and Associated Equipment **869**, 46 (2017), ISSN 0168-9002, 1605.03525.